Journal Pre-proof

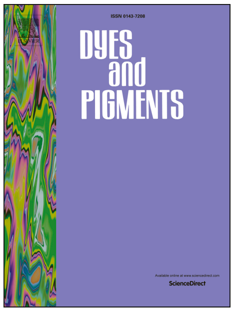

Photodegradation of iron gall ink affected by oxygen, humidity and visible radiation

Yun Liu, Tom Fearn, Matija Strlič

PII: S0143-7208(21)00813-5

DOI: https://doi.org/10.1016/j.dyepig.2021.109947

Reference: DYPI 109947

To appear in: *Dyes and Pigments*

Received Date: 9 August 2021

Revised Date: 12 November 2021

Accepted Date: 13 November 2021

Please cite this article as: Liu Y, Fearn T, Strlič M, Photodegradation of iron gall ink affected by oxygen, humidity and visible radiation, *Dyes and Pigments* (2021), doi: https://doi.org/10.1016/j.dyepig.2021.109947.

Author contributions

Y. L.: conceptualisation, formal analysis, investigation, methodology, software, validation, writing – original draft preparation. T. F.: conceptualisation, methodology, supervision, writing – review & editing. M.S.: conceptualisation, methodology, resources, supervision, writing – review & editing.

Title

Discolouration of iron gall ink affected by oxygen, humidity and visible radiation

Authors

Yun Liu[a,b]*, Tom Fearn[c], Matija Strlič[a,b]

Affiliations

a. Museum Conservation Institute, Smithsonian Institution, Washington D.C., USA.
b. UCL Institute for Sustainable Heritage, University College London, London, UK.
c. Department of Statistical Science, University College London, London, UK.
*Corresponding author. Email: LiuY@si.edu.

Title

Photodegradation of iron gall ink affected by oxygen, humidity and visible radiation

Abstract

The causes of the discolouration of iron gall ink have been debated for decades. As a contribution to the understanding of the photodegradation behaviour of iron gall ink, this paper discusses the effects of three environmental factors that are of primary concern – oxygen, moisture and light. Using a range of historical paper-based samples, a 2^3 full factorial experiment was designed to quantify the effects of oxygen concentration $[O_2]$, relative humidity (RH), illuminance (E_v) of broadband LED light, and their interactions. A change in diffuse reflectance with time was observed to mainly take place beyond 600 nm into the NIR range. The change followed similar patterns under all the experimental conditions, which was modelled by a logarithmic relationship with time of degradation. The rate constant was obtained and was found to be mainly affected by $[O_2]$, RH and their interaction. The role of E_v needs further investigation, however, its insignificant effect on the discolouration measured in this research suggested the possibility of effective degradation control with relaxed lighting controls. Furthermore, the wavelength sensitivity of iron gall ink's discolouration was investigated using narrowband radiation centred at three different wavelengths (Λ): 450 nm ($[\Lambda_{450}]$), 525 nm ($[\Lambda_{525}]$) and 625 nm ($[\Lambda_{625}]$), with varying $[O_2]$ and RH. RH, Λ, the interaction between RH and Λ, and the interaction between RH and $[O_2]$ were found to have strong effect on the rate constant of discolouration. Among these factors, Λ showed the strongest effect, which decreased as Λ increased. Approximately 3x and more than 10x faster degradation by $[\Lambda_{450}]$ than $[\Lambda_{525}]$ and $[\Lambda_{625}]$ respectively was observed, which was likely to be associated with photon energy and quantum efficiency in absorption at different wavelength.

Key words

Discolouration, spectrophotometry, factorial experimentation, iron gall ink, wavelength dependency

List of abbreviations

ANOVA	Analysis of variance
ΔE_{00}	Total colour difference defined by CIEDE2000 formula
ΔE_{00N}	Normalised total colour difference defined by CIEDE2000 formula
E	Photon energy in Joules
E_v	Illuminance in lux
$k_{\Delta E00N}$	Normalised rate constant of change in total colour difference
$k_{\Delta R}$	Rate constant of change in diffuse reflectance
$k_{\Delta RN}$	Normalised rate constant of change in diffuse reflectance
$K_{\Delta RN}$	Normalised rate of change in diffuse reflectance in day^{-1}
LED	Light-emitting diode
N	Number of photons in mol
$[O_2]$	Oxygen concentration

ΔR	Change in diffuse reflectance
ΔR_N	Normalised change in diffuse reflectance
R^2	Coefficient of determination
RH	Relative humidity
SPD	Spectral power distribution
[Λ]	Narrowband radiation centred at Λ
Λ	Wavelength of radiation in nm
λ	Wavelength of reflectance in nm

1. Introduction

The discolouration of iron gall ink-containing collections has been one of the concerns among conservation professionals for decades, but the issue has rarely been investigated by scientific research. It is known that iron gall ink typically undergoes a dramatic colour change from blueish black to brown, mainly due to the oxidation of Fe (II) to Fe (III) by atmospheric oxygen (Perron and Brumaghim, 2009; Díaz Hidalgo *et al.*, 2018), but the process usually takes place shortly after its application. Therefore, the iron gall ink-containing objects in today's collections have already passed this stage and the following stage of discolouration is more relevant to the present collection management. Lighting guidelines for museums, galleries and archives, such as PAS 198 (BSI, 2012), assume that the latter stage of discolouration is induced by light and often categorise iron gall ink as medium sensitive to light.

These statements seem to be made based on a limited number of studies on the discolouration issue of iron gall ink to be found in the literature. These studies are mainly based on conventional light ageing experiments (Reißland and Cowan, 2002) and microfading tests (Tse et al., 2010; Ford, 2014). They all used filtered and unfiltered xenon arc lamps as the light source and the discolouration was assessed by either CIE (Commission Internationale d'Eclairage) colour space (CIELAB) or Blue Wool (BW) Scale (BSI, 2014). Results from different types of samples – artificially degraded model samples (Reißland and Cowan, 2002) and historical samples (Tse *et al.*, 2010; Ford, 2014) were obtained and they are in agreement that iron gall ink is highly sensitive to visible light with the fading rate being equivalent to between BW1 and BW3. Ford (2014) further looked at the effect of environmental factors on the photodegradation processes indicated by the total discolouration defined by CIE (ΔE_{00}) (CIE, 2001; Sharma, Wu and Dalal, 2005). Water vapour was found to have no effect on the rate of change whereas the absence of O_2 was likely to moderately accelerate the discolouration of historical iron gall ink on paper (Ford, 2014).

To understand these observations better in order to build further research upon them, it is necessary to pay attention to the underlying assumptions in these studies. The first assumption is that all the observations represent the behaviours of iron gall ink independent of its support. Although techniques targeting the surface were usually used to take the measurements, it was largely overlooked that the samples being investigated were composite material systems composed of ink and its support, being either paper, parchment or papyrus. Although only the ink layer was of main interest, the support underneath might have inevitably affected the degradation of the ink layer and the data acquisition from the ink layer. This can add complexity to the interpretation of the results.

In fact, the degradation behaviour of iron-containing colourants has been observed to be critically affected by the physicochemical interactions between the colourants and their substrates. Gallotannin dyestuff with iron mordants was observed to be less sensitive to light exposure if not applied on paper (Hofenk de Graaff, Roelofs and van Bommel, 2004). The photoreduction behaviour of Prussian blue (iron(III) hexacyanoferrate(II)) has been found to be dependent on the composition, structure, and photosensitivity of the substrate supporting the pigments (Gervais et al., 2013, 2014, 2015, 2016; Koestler et al., 2018).

In addition to the reactions induced by the condition and characteristics of the substrates, the measured substrate dependence could also be caused by the penetration of radiation through the surface layer of the colourants. The radiation could either be that which induces the photodegradation of the samples, or that which is used to take the measurements for analysis. Although the energy level of visible light is relatively low, it has been found that the energy of photons at wavelengths from 400 nm to 700 nm was sufficient to penetrate through watercolour paint layers and acted evenly throughout the bulk of rag paper (Thomas et al., 2010). This suggests that it was possible that not only the substrate could have degraded independently of the layer of colourants, but also that the measurements could have been mixtures of signals from both the colourants on the surface and the substrate underneath. Only recently, Liu et al. (2021a) showed that for historical iron gall ink-containing documents, in the case where ink application was not exceptionally thin, the reflectance of iron gall ink measured by a hyperspectral imaging system was unlikely to be interfered by the signal from the paper substrates.

The second assumption is that tristimulus colourimetry provides an adequate assessment of the fundamental physicochemical changes in the samples in the discolouration process. It should be noted that although colourimetry is an established analytical method to investigate chemical reactions, there is a difference between the two approaches of colourimetry — spectroscopic colourimetry and tristimulus colourimetry. Spectroscopic colourimetry is commonly used in research on reaction kinetics, when compounds with strong absorption of radiation are involved (Cave and Hume, 1952; Dische, 1953; Hone, Haines and Russell, 2003; Beneto and Siva, 2017). Based on the Beer-Lambert law, absorption of radiation by certain chemical compounds at characteristic wavelengths is usually correlated with the concentration of the reactants to gain insights into the reaction kinetics (Skoog et al., 2012). Tristimulus colourimetry provides a simple and practical method to assess changes in materials at a macro scale due to chemical reactions (Saunders and Kirby, 1994). It is based on the tristimulus parameters that CIE mathematically formulated to describe the trischromatic nature of human vision perceiving reflected radiation in the visible region of the electromagnetic spectrum (400 – 700 nm) (CIE, 2001; Sharma, Wu and Dalal, 2005). In scientific research, CIELAB is the most widely used colour space to assess lightness (L^*) and chromaticity in red-green (a^*) and yellow-blue (b^*), as well as the total colour difference (ΔE) (Saunders and Kirby, 1994; Korifi et al., 2013; Brigham et al., 2018).

Given that $L^*a^*b^*$ and ΔE are obtained by transforming the reflectance of the objects using a set of colourimetric observer functions at a certain observing angle and under a standard CIE illuminant, tristimulus values may not represent the whole picture of the objects' response in reflectance. It has been found that the tristimulus transformation can cause distortion of the quantitative relationships established by spectral analysis (Liu, Fearn and Strlič, 2021c). If robust correlations between the tristimulus parameters and the analytes of interest can be established, change in chemical reactions can be quantified (Gray and Wright, 1964; Rosu, Rosu and Cascaval, 2009). However, such correlations are still absent for the ink-paper system. On the other hand, CIE L*a*b* and ΔE has been applied to assess the degradation of the ink-paper system (Reißland and Groot, 1999; Reißland and Cowan, 2002; Tse et al., 2010; Ford, 2014). These results provide significant information to the preservation of the ink-containing objects. But if insights into the chemical processes of the degradation of iron gall ink are to be gained based on these results, data obtained through more objective methods, such as spectroscopic colourimetry, needs to be further examined.

The third assumption that has often been taken for granted is that the photodegradation of iron gall ink is dominated by illuminance. This often leads to an exclusive attention on illuminance in collection management. In practice, lux hours, i.e. illuminance multiplied by time, is commonly used as a measure to control the degradation of light sensitive materials (Blades et al., 2017). The emphasis on illuminance can cause neglect of the effects of other external and internal factors, such as temperature, oxygen, humidity, radiation wavelength, presence of photosensitisers, and the material compositions, which are otherwise identified as the most important driving forces in photochemical reactions. Among all the factors other than illuminance, oxygen has been the most studied environmental factor in the research on pigments and dyes. It has been found that anoxia and hypoxia can benefit the majority of the unstable colourants (Lerwill *et al.*, 2015), except for metal-containing colourants (Villmann and Weickhardt, 2021). Furthermore, Ford (2014) seems to be the only research that has taken the effect of RH into consideration but did not observe a significant effect of RH on the discolouration of iron gall ink. No research that has investigated the interactions between different factors has been reported in the English literature.

To elucidate these ambiguities related to the discolouration of iron gall ink and to support preventive conservation of historical iron gall ink-containing collections, the discolouration behaviour of iron gall ink affected by the environmental factors—light, humidity and oxygen was investigated in this research. Given the diverse and uncertain nature of the iron all ink-containing objects in the collections due to te raw materials, production and the degradation processes, historical documents were used as samples to best represent the iron gall ink-containing objects in real collections, thus the results can be relevant to preventive conservation in practice. As an efficient way to quantify the synergistic effect of these three factors, we designed and carried out factorial experiments to examine the main effects and the interactions between the factors on discolouration. Spectroscopic colourimetry was used as a direct measurement method to assess the sample response and the results were compared with tristimulus values. Continuous and narrow band visible radiation were used as light sources to gain insights into the role of illuminance on the discolouration of iron gall ink, which led to improved suggestions for resource distribution in collection management.

2. Methodology

2.1 Samples

Twenty-five sacrificial historical samples of iron gall ink containing rag paper (18th—20th century) were collected through purchases from online retailers and donations from The National Archives (Kew, UK). These samples are not an exhaustive representation of the history, but they cover a wide range of ink and paper variations in composition and application by visual examination. Each sample was divided into 1.0 cm x 1.5 cm rectangular subsamples. It was ensured that each subsample contained similar amounts of ink application and stained areas were avoided. Among these 25 samples, 23 were used for the experiment under broadband visible radiation and five samples were used for the experiment designed to explore the wavelength-dependent degradation (three of the 25 samples were used for both experiments) (Figure 1).

(a)

(b)

Figure 1. Samples used for the experiments under (a) broadband radiation and (b) narrowband radiation. Three samples, i.e. #34, #35 and # 98 were used for both experiments.

2.2 Experimental setup

All of the experimental runs were carried out in the reaction chamber as shown in Figure 2, which was modified from the setup designed by Liu et al. (2021c). Gas supplies were regulated to achieve desired oxygen concentration ([O_2]) (v/v %) by an Aalborg GFC aluminium body mass flow controller (Caché Instrumentation, UK). The gas mixture then flowed through a V-GenTM Dew Point/RH Generator (InstruQuest Inc., US) to regulate the humidity level for the desired relative humidity (RH) in the reaction chamber. The desired atmospheres were continuously circulated at 200 ml·min^{-1} through the systems 24 h before and during the irradiation. A Light-emitting diode (LED) light bulb (240 V, 13 W, 1521 lm, Philips, Netherlands) was used as the broadband radiation source. The spectral power distribution (SPD) of the LED (Figure 2) was measured using a GL SPECTIS 1.0 spectrometer (GL Optic, Poland-Germany).

For the broadband irradiated degradation, the 23 subsamples were attached to a ring of Whatman filter paper No. 1 (Figure 1a) and hung in the chamber supported by the sample holder. For the wavelength-dependent degradation, the five subsamples were attached to a piece of Whatman filter paper No. 1

(Figure 1b) and hung behind the bandpass filters. The bandpass filters passed radiation (bandwidth ≈ 55 nm) centred at 450 nm ([Λ_{450}]) (XNiteBP450, LDP LLC, US), 525 nm ([Λ_{525}]) (XNiteBP525, LDP LLC, US) and 625 nm ([Λ_{625}]) (XNiteBP625, LDP LLC, US) (Figure 3). The temperature (T) was kept at 21 °C throughout the experimental runs and the environmental conditions inside the chamber were constantly monitored by HOBO Data Loggers (U12-012, Tempcon Instrumentation, UK).

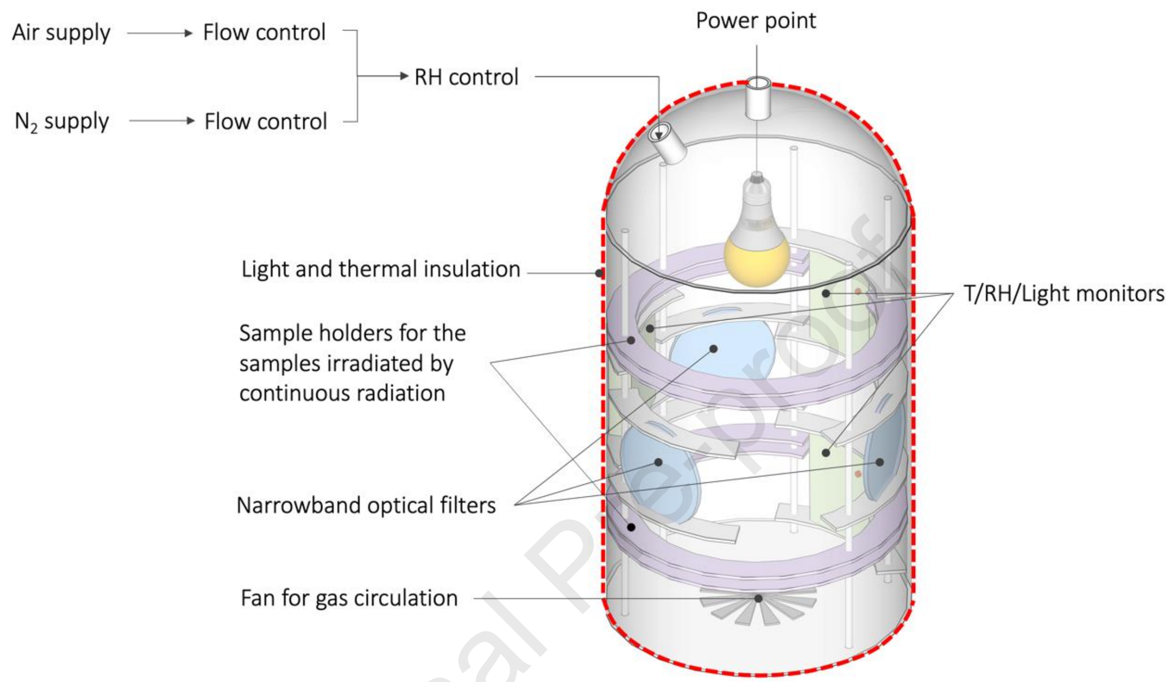

Figure 2. Diagram showing the setup of the reaction chamber for the accelerated photodegradation experimental runs.

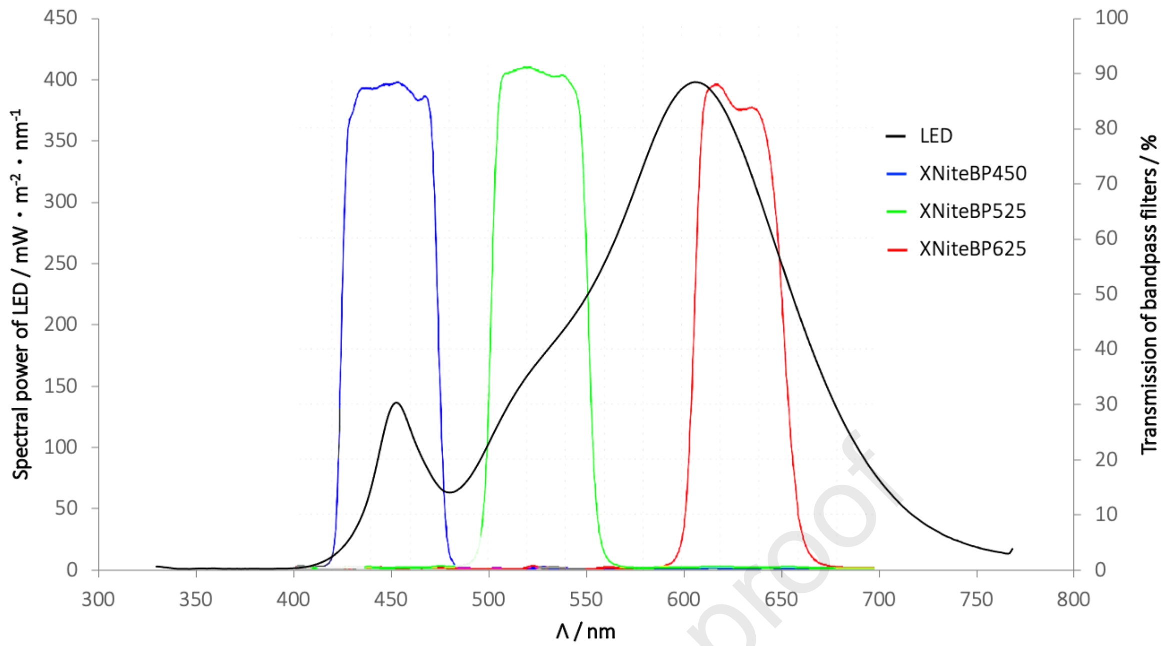

Figure 3. The spectral power distribution (SPD) of the LED light source (black line) and the profiles of the three bandpass optical filters used in the experimental setup (Liu, Fearn and Strlič, 2021c). The SPD shown was measured at the position of the high sample holder.

2.3 Experimental design

To maximise the efficiency in time and resources, the experiments using broadband radiation and narrowband radiation were carried out in the reaction chamber simultaneously. Therefore, a total of four experimental runs were carried out, each run containing five sets of subsamples, with different illumination being achieved by positioning and the use of narrowband optical filters. The specifications of the experimental runs and the combinations of the conditions are presented in Table 1. The range of [O_2] was chosen the represent the typical level in an anoxic display encasement and in an atmospheric environment. The range of RH was chosen based on the recommended environmental targets in museums and libraries by ICOM-CC and IIC (40 – 60%) (ICOM-CC and IIC, 2014), Smithsonian Institution Archives (30 – 50%) (Smithsonian Institution Archives, no date), and PAS 198 (35 – 60%) (BSI, 2012) with ± 10%. A range exaggerated from the values typically used in real scenarios was chose for E_v to obtain measurable results within a practical timeframe for research.

The broadband irradiated degradation under the effect of [O_2] (v/v %), RH (p/p %) and illuminance (E_v) (lx) was investigated in a 2^3 full factorial experiment. In this experiment, each of the three factors took values at two different levels and the experimental runs took on all possible combinations of these levels across all the factors (Grove and Davis, 1992). The order of the designed runs of the factorial experiment was randomised, however, two designed runs where [O_2] and RH were at the same levels were carried out at the same time, together with one set of wavelength-dependent degradation using [Λ_{450}], [Λ_{525}], and [Λ_{625}].

Table 1. The combinations of conditions used for each experimental run in the factorial experiments.

<table>
<tr><th rowspan="2">Experimental run number</th><th colspan="3">Broadband irradiated degradation</th><th colspan="3">Wavelength-dependent degradation</th></tr>
<tr><th>[O_2] %</th><th>RH %</th><th>E_v (lx)</th><th>[O_2] %</th><th>RH %</th><th>Λ (nm)*</th></tr>
<tr><td rowspan="3">1</td><td>21</td><td>20</td><td>5000</td><td rowspan="3">21</td><td rowspan="3">20</td><td>450</td></tr>
<tr><td rowspan="2">21</td><td rowspan="2">20</td><td rowspan="2">20000</td><td>525</td></tr>
<tr><td>625</td></tr>
<tr><td rowspan="3">2</td><td>0</td><td>20</td><td>5000</td><td rowspan="3">0</td><td rowspan="3">20</td><td>450</td></tr>
<tr><td rowspan="2">0</td><td rowspan="2">20</td><td rowspan="2">20000</td><td>525</td></tr>
<tr><td>625</td></tr>
<tr><td rowspan="3">3</td><td>0</td><td>70</td><td>5000</td><td rowspan="3">0</td><td rowspan="3">70</td><td>450</td></tr>
<tr><td rowspan="2">0</td><td rowspan="2">70</td><td rowspan="2">20000</td><td>525</td></tr>
<tr><td>625</td></tr>
<tr><td rowspan="3">4</td><td>21</td><td>70</td><td>5000</td><td rowspan="3">21</td><td rowspan="3">70</td><td>450</td></tr>
<tr><td rowspan="2">21</td><td rowspan="2">70</td><td rowspan="2">20000</td><td>525</td></tr>
<tr><td>625</td></tr>
</table>

*The unfiltered illuminance value received by the subsamples was 18000 lx. The actual energies received by the subsamples were calculated and are discussed later in Results and discussion.

2.4 Data collection

For the experiment runs using either broadband or narrowband radiation, spectroscopic responses in diffuse reflectance were measured for each sample before and during degradation. The first measurement was taken at 0.12 day on average and the subsequent measurements were taken at intervals of 1 – 5 days. The hyperspectral imaging (HSI) technique was used to measure reflectance, particularly for its high spatial resolution, which allowed precise data acquisition from fine ink lines. The HSI system (Camlin, Lisburn, UK) used in this experiment was equipped with a VNIR camera (spectral range: 400 – 1000 nm, spectral resolution: 2 nm) coupled with XENOPLAN 2.8/50-0902 lens (Schneider-KREVZNACH, Germany) and a halogen light source (manufacturer unknown). Dark calibration was carried out with the lens capped, and white calibration was carried out using a Florilon™ Standard (EFWS-99-02c, Avian Technologies LLC, US). The scanning speed (0.8 mm·s^{-1}) was determined in relation to the exposure time (50 ms) and the aperture size (f/5.6) of the camera to obtain square pixels. The spatial resolution of the images was 625 ppi.

2.5 Data processing

After data collection, the pixels of the hyperspectral images of iron gall ink were first spatially separated from paper using k-means clustering with cosine distance metric on spectra from 420 – 870 nm. Examples of the results of the pixel separation are shown in Figure 4. The arithmetic mean spectrum of each ink cluster was calculated to represent the reflectance spectrum of ink for each subsample. No further separation of the reflectance signal from the stratified layers of paper and ink was carried out.

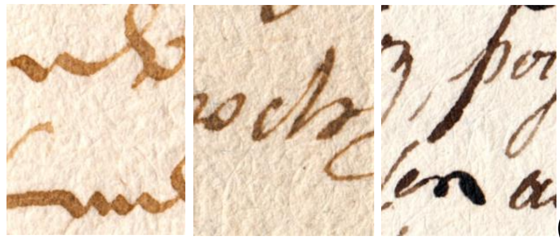
(a)


(b)

Figure 4. Comparison of (a) historical samples of different types of paper with iron gall ink and (b) the separation of pixels of ink from pixels of paper into binary images using k-means clustering over 420—870 nm.

Based on the radiation sources, i.e., broadband radiation (LED) and narrowband radiation [Λ_{450}], [Λ_{525}] and [Λ_{625}], a data cube was constructed for each experimental condition as specified in Table 1. A total of 12 data cubes of reflectance were obtained, where the horizontal axis represented the wavelength (λ) range of interest (424 – 853 nm), the vertical axis represented the samples, and the depth axis represented the time of degradation. Mean data cubes of average reflectance were constructed by averaging the reflectance across all samples for each experimental condition, resulting a total of 4 mean data cubes for each type of radiation (broadband, [Λ_{450}], [Λ_{525}] and [Λ_{625}]), where the first dimension represented the experimental condition, the second dimension represented λ, and the third dimension represented the time of degradation t.

It is worth noting that in this paper, Λ is used to indicate the wavelength of the radiation sources, and λ is used to indicate the wavelength at which the diffuse reflectance was measured. All the data processing and analyses were carried out in MATLAB® R2017a.

3. Results and discussion

3.1 Discolouration under broadband radiation

The change in diffuse reflectance of ink decreased over time as λ increases and was mainly detected at λ > 600 nm (Figure 5). The change in diffuse reflectance (ΔR, day^{-1}) was calculated for each subsample by subtracting the reflectance spectrum before degradation (R_0) from the reflectance spectrum collected at each time interval (R_t) as $\Delta R = R_t - R_0$. The spectra of ΔR were smoothed using Savitzky–Golay filtering (2nd order polynomial, window width 19) (Savitzky and Golay, 1964). Ten representative λs at ~50 nm intervals were selected for further analyses of the rate of change.

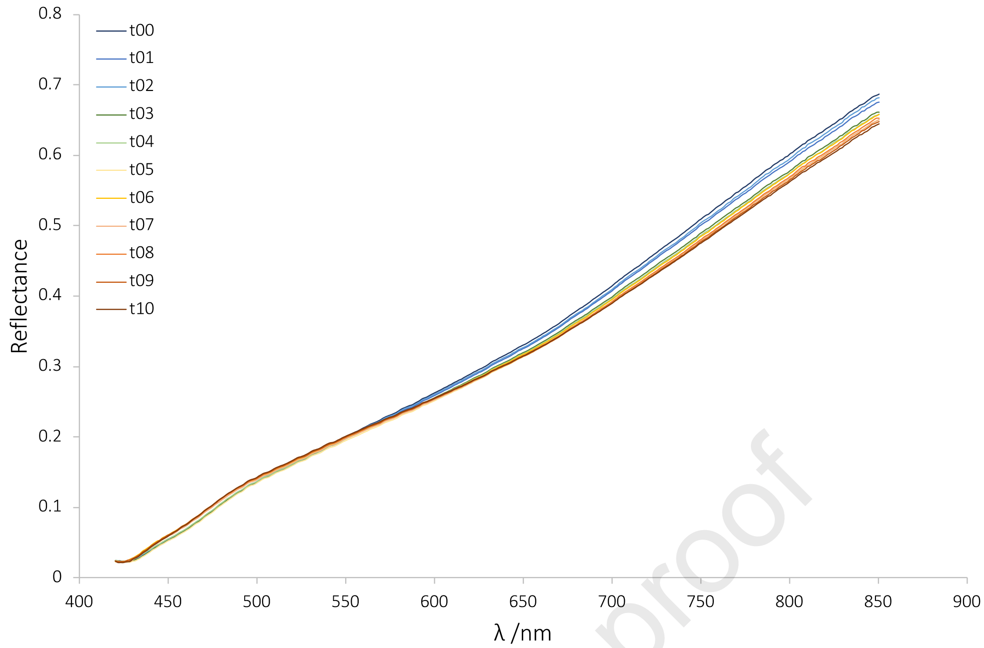

Figure 5. The change of diffuse reflectance that was averaged across the 23 samples degraded at 21% [O2], 70% RH and 20000 lx over time.

The progress of ΔR mainly took place in the first 10 days for all the experimental conditions (Figure s1). The relationship between ΔR and time (t/day) was approximated using a logarithmic relationship:

$$\Delta R = \begin{cases} 0, & t = 0 \\ A_0 + k_{\Delta R} \ln t, & t \geq 0.12 \end{cases} \text{[1]},$$

where A_0 represents the amount of change in reflectance that takes place in a day and $k_{\Delta R}$ represents the rate constant defined by the rate function of ΔR:

$$K_{\Delta R} = d\Delta R\,(dt)^{-1} = k_{\Delta R} t^{-1}, t \geq 0.12 \text{ [2]},$$

where $K_{\Delta R}$ represents the rate of change in ΔR. The logarithmic relationship between ΔR and t implies a very fast initial change in reflectance at all λs for ink.

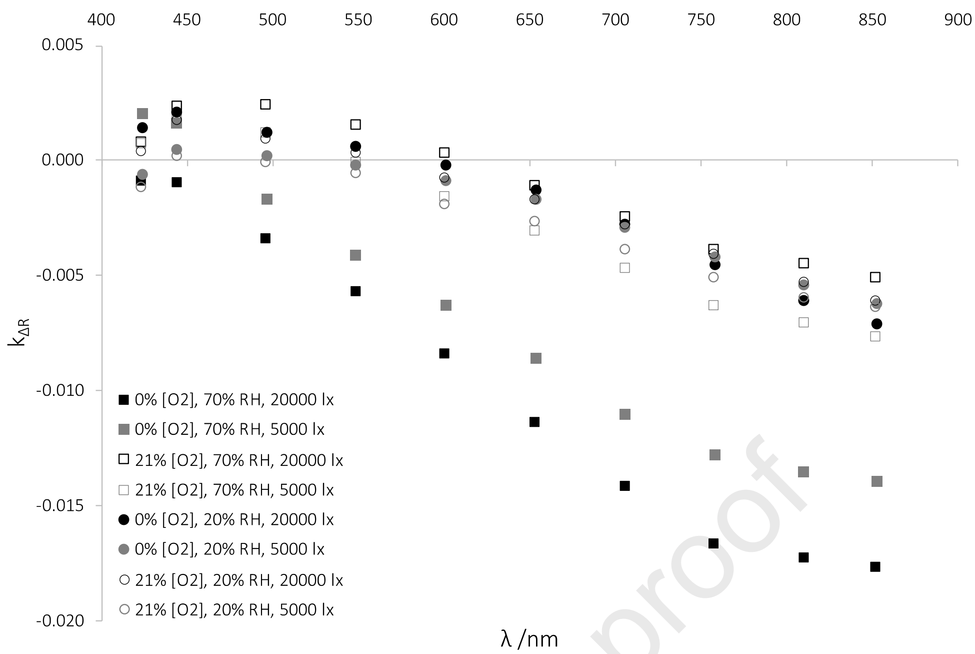

Figure 6. The relationship between the rate constant of discolouration ($k_{\Delta R}$) and the wavelength of reflectance (λ) under different experimental conditions.

$k_{\Delta R}$ was obtained based on the logarithmic approximation (Table s1). A clear relationship between $k_{\Delta R}$ and λ was observed (Figure 6), where $k_{\Delta R}$ decreased as λ increases. This relationship was found nearly linear, with gentle curvature observed in the NIR range for most experimental conditions, suggesting $k_{\Delta R}$ is likely to level off at longer λ beyond 853 nm. Low [O_2] and high RH was observed to have induced the largest absolute $k_{\Delta R}$, suggesting the discolouration of iron gall ink is likely to be promoted in an anoxic and humid environment. The promotional effect of anoxia on discolouration has been observed not only for historical iron gall ink in another independent research (Ford, 2014), but also for another iron-containing pigment – Prussian blue (Del Hoyo-Meléndez and Mecklenburg, 2011; Lerwill *et al.*, 2015; Koestler *et al.*, 2018). Research on the chemistry of Prussian blue reveals that its colour intensity arises from the charge transfer transition from Fe (II) to Fe (III) in the Fe (III) – N – C – Fe (II) moiety (Kirby and Saunders, 2004). Anoxia may interrupt this configuration thus lead to discolouration. Similarly, iron gall ink has been found contain mixed-valence transition metal complexes (Rouchon *et al.*, 2011). Anoxia can in principle cause charge transfer transition from Fe (III) to Fe (II) that leads to the observed shifts in reflectance.

Prior to quantify the effects of [O_2], RH and E_v by analysis of variance (ANOVA), a half-normal probability plot, which is used to assess the statistical significance of effects in a factorial experiment without replications (Daniel, 1959), was used to screen the effects. The half-normal plot for $k_{\Delta R}$ at 811 nm ($k_{\Delta R\text{-}811}$) is shown in Figure 7. A clear break was observed between two groups – one includes [O_2], RH, and [O_2]*RH, and the other includes E_v, RH*E_v, [O_2]*E_v and [O_2]*RH*E_v. [O_2], RH, and [O_2]*RH show similar absolute effect values that deviate from the line of null effect, suggesting that the effects of [O_2], RH and their interaction were likely to be distinctively stronger than the effects involving E_v. This provides a reasonable justification to include the effects involving E_v in the error estimate for ANOVA.

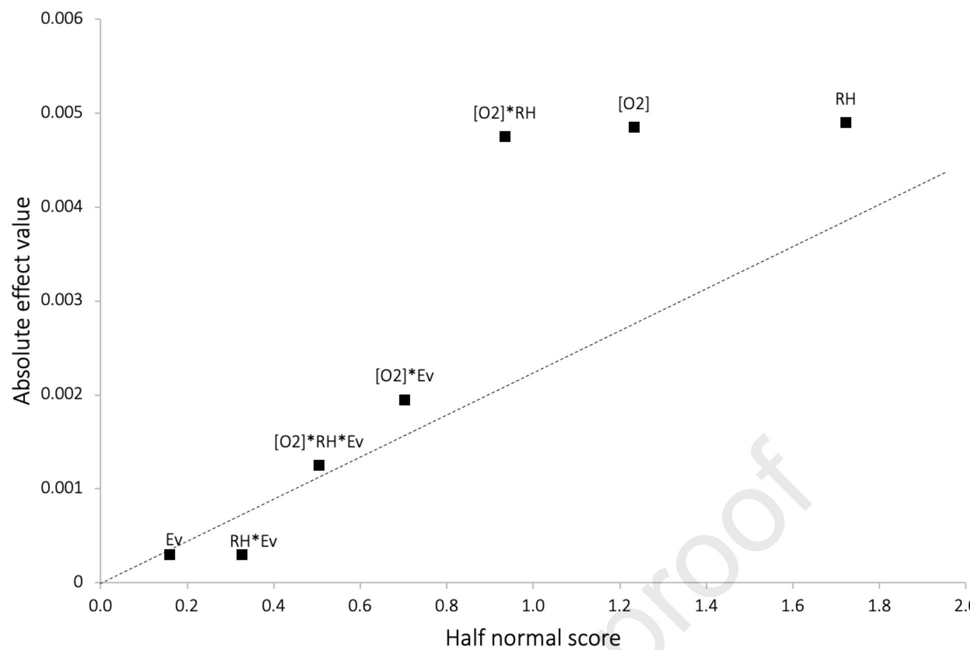

Figure 7. Half normal plot for the effects of $[O_2]$, RH, E_v and their interactions on the rate constant of change in reflectance at 811 nm of iron gall ink. The dashed line represents the line of null effect.

Based on the half normal plot, ANOVA was carried out and the results for $k_{\Delta R\text{-}811}$ are summarised in Table 2. As shown in the table, $[O_2]$, RH and their interaction were found to have similarly strong and significant effect (p-value < 0.05), which is consistent with what Figure 7 suggests. Therefore, it is plausible to conclude that the discolouration of iron gall ink under broadband visible radiation was mainly affected by $[O_2]$, RH and their interaction, whereas the effect of E_v and its interaction with the other factors were relatively weak and could be negligible. The observed weak effect of E_v on $k_{\Delta R}$ suggests that putting illuminance as the central focus may not be the most effective strategy to manage the discolouration of iron gall ink-containing paper collections. But this does not mean light does not play a role. Studies on Prussian blue pigments suggest that light could be essential to initiate the discolouration of iron-containing pigments in anoxia (Koestler *et al.*, 2018). More experiments need to be designed to gain insights into the role of illuminance in the discolouration processes of iron gall ink.

Table 2. ANOVA of the effects of $[O_2]$, RH and their interaction on $k_{\Delta R\text{-}811}$.

Source	Sum of squares	Degree of freedom	Mean square	F	p-value
$[O_2]$	4.70E-5	1	4.70E-5	16.97	0.0146
RH	4.80E-5	1	4.80E-5	17.32	0.0141
$[O_2]$*RH	4.51E-5	1	4.51E-5	16.28	0.0157
Residuals	1.11E-5	4	2.77E-6		

Analyses of the reflectance spectra in CIE LAB colour space revealed that the tristimulus total colour change ΔE_{00} (CIE, 2001; Sharma, Wu and Dalal, 2005) followed a logarithmic pattern of progression over time (Liu, Fearn and Strlič, 2021a). Consistent results of ANOVA were also obtained, where $[O_2]$, RH and their interaction were found to have significant impact on ΔE_{00} (Liu, Fearn and Strlič, 2021a). For the duration of the experiment, ΔE_{00} remained below 2.0 for most experimental runs. Only the samples degraded at 0% [O_2] and 70% RH reached above ΔE_{00} 4.0. Since human perception of colour change varies according to the material and environmental contexts (Mahy, Van Eycken and Oosterlinck, 1994; Johnston-Feller, 2001), it is difficult to assess the perception of the discolouration of iron gall ink by unaided human vision based on the available data. Particularly, the iron gall ink studied in this research, as well as in many other historical objects, is undetachable from the background which is likely to undergo discolouration as the ink discolours (Liu, Fearn and Strlič, 2021b, 2021c). How the simultaneous change of ink and its substrate influences the noticeability of any change in ink has not been studied and deserves an independent research project in the future.

It is worth noting that given the nature of historical samples, there may be a large variability among the ink samples due to ink compositions and the degradation products (Kolar et al., 2006). Comprehensive characterisation of the ink samples may be helpful for the interpretation of the results, although it can be extremely challenging since the original recipes and manufacturing processes are usually unknown. In addition, had more resources been available, more definite results might have been obtained by carrying out replications of the experimental runs for more accurate estimates of both the error variance and the effects.

3.2 Wavelength-dependent discolouration

Given that [Λ_{450}], [Λ_{525}], and [Λ_{625}] were generated using bandpass filters with a broadband LED radiation source which has non-uniform power distribution across Λ (Figure 2), normalisation was carried out prior to all the analyses. The number of photons (N, $mol\cdot s^{-1}\cdot m^{-2}$) received by the subsamples was calculated based on the Planck-Einstein relation:

$$N = \Lambda E(N_A hc)^{-1} \text{ [3]},$$

where Λ is the wavelength of the radiation in nm, E is the total photon energy reaching a subsample surface in $J\cdot s^{-1}\cdot m^{-2}$, N_A is Avogadro's constant in mol^{-1}, h is the Planck constant in J·s and c is the speed of light in $m\cdot s^{-1}$. E was measured using GL SPECTIS 1.0 (GL Optic, Poland-Germany) at the position of the samples. Under the assumption that the number of photons that were absorbed and led to investigated photodegradation in the subsamples was proportional to the number of photons that irradiated the subsamples, the normalised change in reflectance (ΔR_N) for each [Λ] was calculated as:

$$\Delta R_N = N^{-1}\Delta R \text{ [4]},$$

where ΔR is the change in diffuse reflectance as measured by the hyperspectral imaging system at each time interval during the degradation of iron gall ink. Based on Equations 1 and 2, the normalised rate constant of change in diffuse reflectance ($k_{\Delta RN}$) was calculated over 424 – 853 nm at approximately 50 nm intervals for the subsamples exposed to [Λ_{450}] ($k_{\Delta RN\text{-}B}$), [Λ_{525}] ($k_{\Delta RN\text{-}G}$) and [Λ_{625}] ($k_{\Delta RN\text{-}R}$) (Table s2). The relationship between $k_{\Delta RN}$ and λ in different environmental conditions was plotted in Figure 8 for [Λ_{450}] (Figure 8a), [Λ_{525}] (Figure 8b) and [Λ_{625}] (Figure 8c). These plots clearly demonstrate that all the narrowband radiation induced spectroscopic response across the full range of λ. Faster change took place at long λ, mainly in the NIR range. $k_{\Delta RN}$ decreased as λ increased, resulting in the largest amount of change at the red end of the spectrum. These observations are consistent with those made with broadband LED radiation. Curvature was observed at both ends of the spectral range in the relationship between $k_{\Delta RN}$ and λ. The curvature at the low end is likely due to the low signal to noise ratio whereas that at the high end may indicate the levelling off trend of $k_{\Delta RN}$ at λ beyond 850 nm.

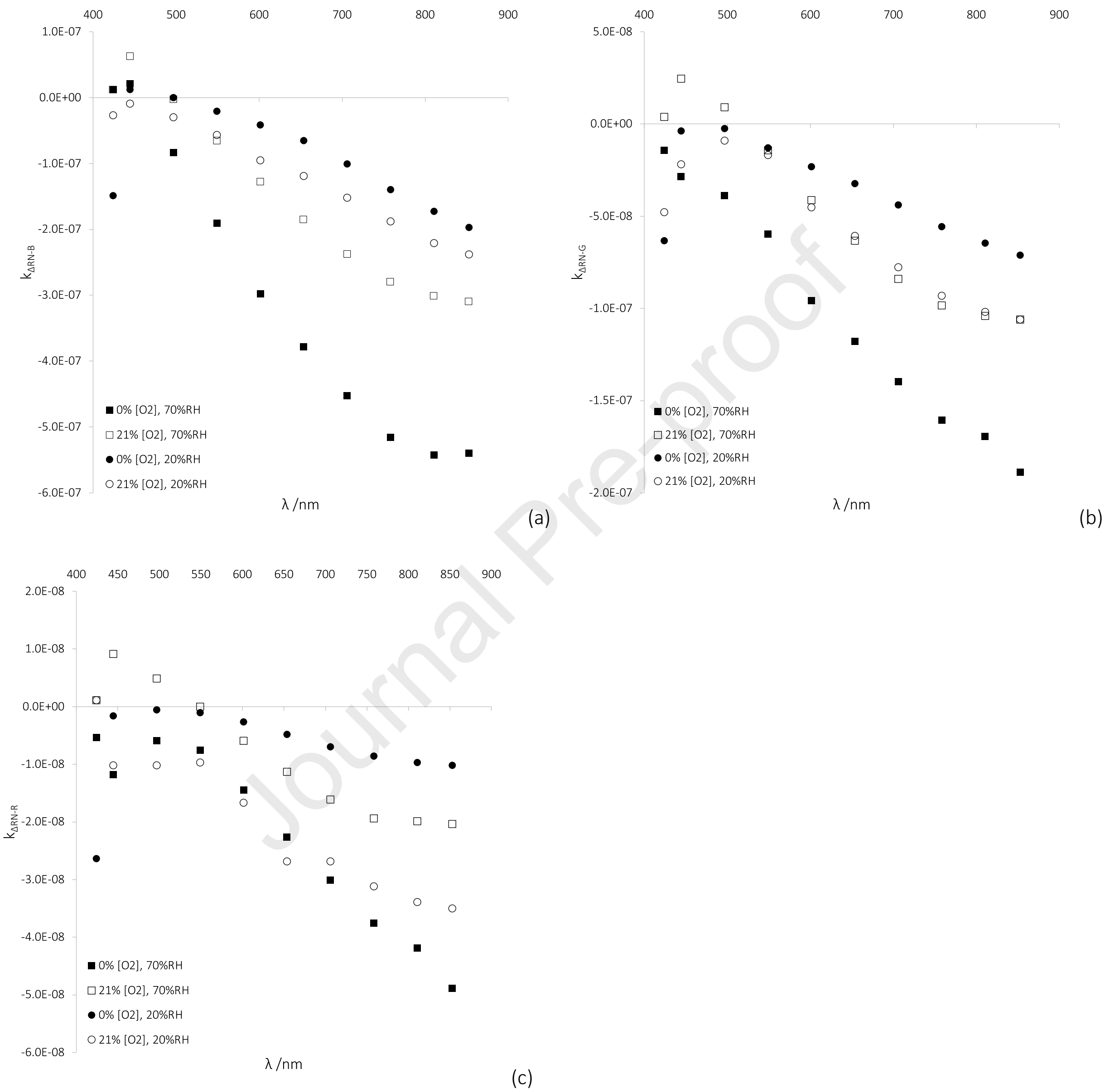

Figure 8. The relationship between $k_{\Delta RN}$ and λ for samples exposed to: (a) [Λ_{450}], (b) [Λ_{525}], and (c) [Λ_{625}]. It is worth noting that the y-axis scale is very different in the three figures.

The dependence of $k_{\Delta RN}$ on Λ in different experimental conditions was further explored. Similar trends of the relationship were observed across λ and the result of $k_{\Delta RN-811}$ is shown in Figure 9. Figure 9a clearly shows that [Λ_{450}] induced the fastest change in diffuse reflectance across all the experimental conditions. As Λ increases, $k_{\Delta RN-811}$ decreased. Figure 9b shows that the relationship between $k_{\Delta RN-811}$ and photon energy was not linear and can be complex. More data are needed to establish a comprehensive picture of the relationship between the rate constant and photon energy. Further analysis of the pairwise relationships between $k_{\Delta RN\text{-}B}$, $k_{\Delta RN\text{-}G}$ and $k_{\Delta RN\text{-}R}$ revealed that these relationships were nearly linear for each environmental condition and the coefficients of proportionality were found to be similar for different conditions (Figure 10a). On average, $k_{\Delta RN\text{-}B}$ was found to be approximately 3.1 times and 9.7 times as much as $k_{\Delta RN\text{-}G}$ and $k_{\Delta RN\text{-}R}$, respectively. This confirms that not only the photon energy played a role in affecting $k_{\Delta RN}$, but also that other factors such as quantum efficiency need to be considered in further causal analysis.

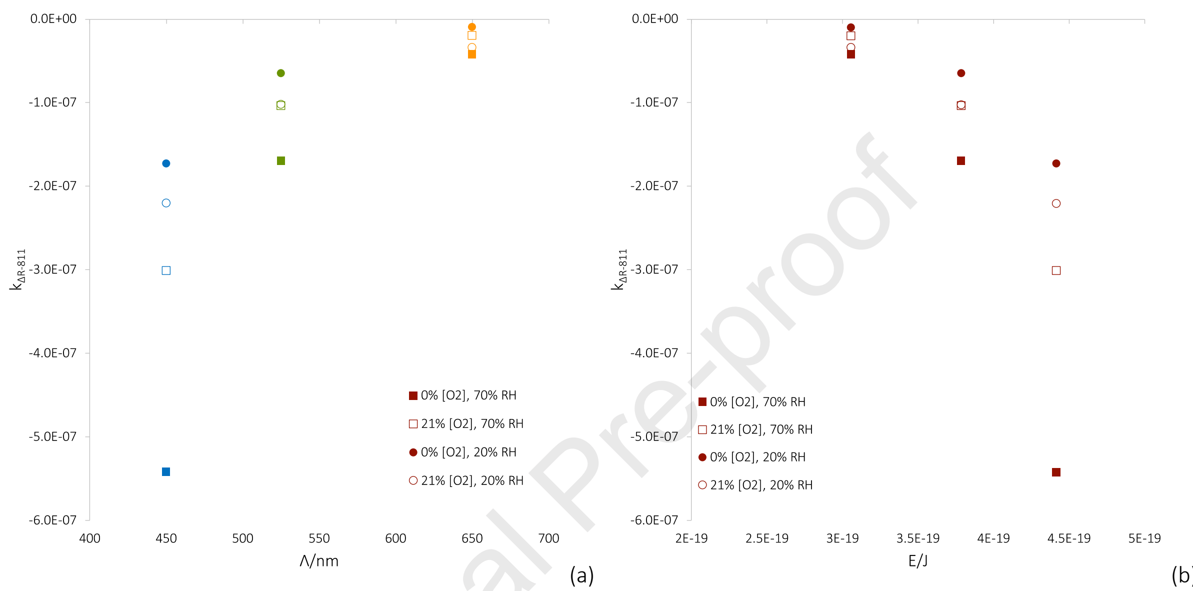

Figure 9. (a) The dependence of $k_{\Delta RN\text{-}811}$ on Λ under different experimental conditions. (b) The non-linear relationship between $k_{\Delta RN\text{-}811}$ and photon energy (E).

In addition to the effect of Λ, the effect of RH was also observed. As shown in Figure 8 and 9, for subsamples exposed to each [Λ], the fastest and the slowest change in reflectance was achieved at 70% RH and 20% RH respectively, suggesting RH was likely to drive the rate of change in reflectance of iron gall ink. The higher the RH the stronger the effect. Furthermore, although the effect of $[O_2]$ was not evident in the plots, an interaction between RH and $[O_2]$ emerged. Figure 8 (a) clearly shows that when RH was high, $k_{\Delta RN}$ was inhibited by the presence of O_2, whereas at low RH, $k_{\Delta RN}$ was promoted by O_2.

These observations of the effects of Λ, RH, and $[O_2]$ were validated by ANOVA. Under the assumption that the three-factor effect was negligible, ANOVA was carried out for $k_{\Delta RN}$ at 811 nm ($k_{\Delta RN\text{-}811}$). The results of ANOVA are presented in Table 3. As expected, Λ showed the strongest effect on $k_{\Delta RN\text{-}811}$ and RH showed the 2nd strongest effect, followed by the interaction between RH and $[O_2]$ and the interaction between RH and Λ. Although the p-values of the effects of RH, RH*$[O_2]$, and RH*Λ were found larger than 0.05, these effects were still considered possibly significant since their F-values were evidently larger than the other factors. As noted earlier, a clearer picture could be obtained with more precise estimation of the effects and increased confidence in the magnitude of the errors through replication of the experimental runs. Given that much of the change of the samples happened in the first two weeks, the replication would take a shorter time span, which would make it more feasible.

Table 3. ANOVA for the effects of $[O_2]$, RH, Λ and their interactions on $k_{\Delta RN\text{-}811}$.

Factors	Sum of squares	Degree of freedom	Mean square	F-value	p-value
$[O_2]$	4.01E-15	1	4.01E-15	1.00	0.42
RH	2.75E-14	1	2.75E-14	6.83	0.12
Λ	1.69E-13	2	8.45E-14	20.97	0.04
$[O_2]$*RH	1.60E-14	1	1.60E-14	3.98	0.18
$[O_2]$*Λ	5.51E-15	2	2.75E-15	0.68	0.59
RH*Λ	2.59E-14	2	1.29E-14	3.21	0.24
Error	8.06E-15	2	4.03E-15		

The analyses of the reflectance spectra in the CIE LAB space revealed that the progression of normalised ΔE_{00} (ΔE_{00N}) also followed a logarithmic trend (Figure s2) and the rate constant of ΔE_{00N} ($k_{\Delta E00N}$) was obtained for $[\Lambda_{450}]$ ($k_{\Delta E00N\text{-}B}$), $[\Lambda_{525}]$ ($k_{\Delta E00N\text{-}G}$) and $[\Lambda_{625}]$ ($k_{\Delta E00N\text{-}R}$). Qualitatively, results that are consistent with the spectroscopic analyses were obtained, where ΔE_{00N} was found to be inversely proportional to Λ, the relationship between $k_{\Delta E00N}$ and Λ^{-1} was found to be nonlinear, and Λ was found to predominantly affect the discolouration. However, the tristimulus transformation seemed to have affected the quantitative relationships between $k_{\Delta E00N\text{-}B}$, $k_{\Delta E00N\text{-}G}$ and $k_{\Delta E00N\text{-}R}$. As shown in Figure 10b, $k_{\Delta E00N\text{-}B}$ was found to be approximately 2.5 times and 6.3 times as much as $k_{\Delta E00N\text{-}G}$ and $k_{\Delta E00N\text{-}R}$, respectively, which is slightly different from the proportionality between $k_{\Delta RN\text{-}B}$, $k_{\Delta RN\text{-}G}$ and $k_{\Delta RN\text{-}R}$, as shown in Figure 10a. The tristimulus transformation was found to have reduced the relatively strength of $[\Lambda_{450}]$ to $[\Lambda_{525}]$ and $[\Lambda_{625}]$ by approximately 19% and 35%, respectively. These differences seem to be a systematic distortion caused by the tristimulus transformation. Further investigations into the formula are needed to gain insights.

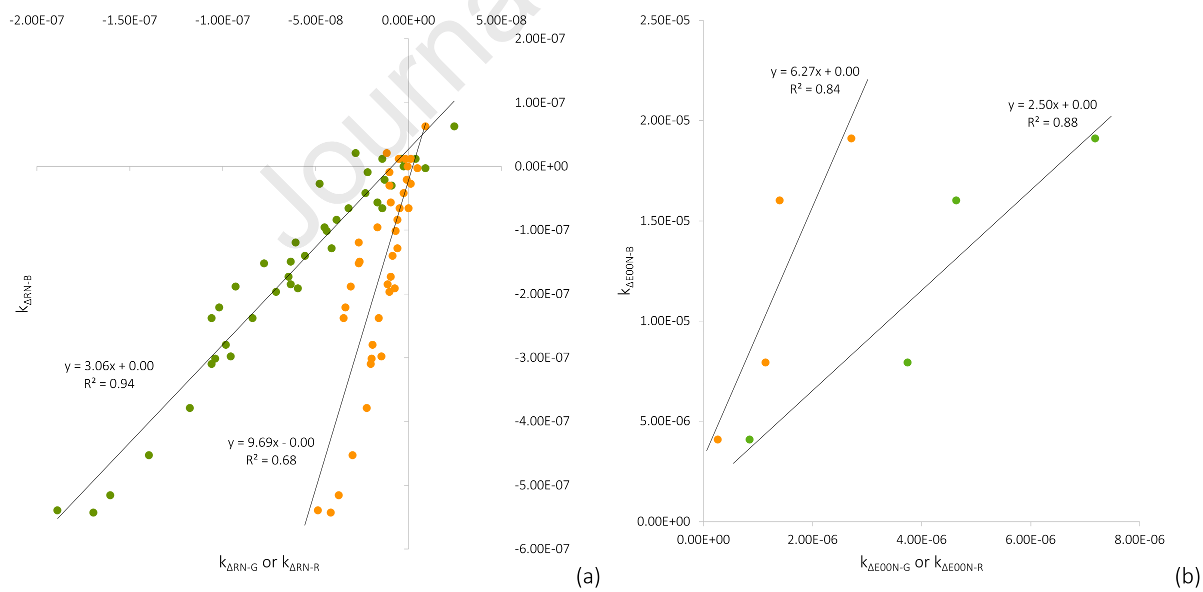

Figure 10. Comparison between the effects of $[\Lambda_{450}]$, $[\Lambda_{525}]$ and $[\Lambda_{625}]$ on $k_{\Delta RN}$ and $k_{\Delta E00N}$. (a) The relationship between $k_{\Delta RN\text{-}B}$ and $k_{\Delta RN\text{-}G}$ (green) and between $k_{\Delta RN\text{-}B}$ and $k_{\Delta RN\text{-}R}$ (orange). (b) The relationship between $k_{\Delta E00N\text{-}B}$ and $k_{\Delta E00N\text{-}G}$ (green) and between $k_{\Delta E00N\text{-}B}$ and $k_{\Delta E00N\text{-}R}$ (orange).

4. Conclusions

This research aimed to provide scientific insights into the discolouration of iron gall ink on paper, which has long been debated among heritage scientists. A 2^3 full factorial experiment was designed and carried out to investigate the effects of $[O_2]$, RH, and E_v of broadband visible radiation on the photodegradation of iron gall ink. A comprehensive understanding of the spectroscopic responses of iron gall ink was achieved by monitoring ΔR before and during degradation. Within the range of λ investigated in this experiment (424 – 853 nm), ΔR was mainly observed at λ > 600 nm. ΔR decreased as λ increased beyond 600nm, leading to a larger amount of change achieved in the near infrared spectral range.

ΔR followed logarithmic relationships with time and the rate constant $k_{\Delta R}$ was obtained. The significance of $[O_2]$, RH, $E_{v,}$ and their interactions on $k_{\Delta R}$ at 811 nm was analysed by ANOVA and a half normal probability plot. Although no clear-cut results were obtained, $[O_2]$, RH, and $[O_2]$*RH were shown to have stronger effects and were considered to be adequate to predict the discolouration of iron gall ink for collection management. This result revealed that the role of E_v was not as significant as had been thought in collection management. Given that the E_v variation in the experiment is much bigger that in a real scenario, whereas the $[O_2]$ and RH variations are more realistic, the effect of E_v is likely to be considerably weaker compared to $[O_2]$ and RH in reality. This suggests that a more in-depth investigation into the effect of $[O_2]$ and RH is needed, whereas more relaxed and flexible guidelines for illumination and light exposure can be adequate to manage the discolouration of iron gall ink containing works.

In addition, the wavelength sensitivity of the photodegradation behaviours of iron gall ink was explored using narrowband radiation $[\Lambda_{450}]$, $[\Lambda_{525}]$ and $[\Lambda_{625}]$. Normalised rate constant, $k_{\Delta RN}$ in per mole of photons, was obtained. Λ was observed to have the strongest effect on $k_{\Delta RN}$, where $k_{\Delta RN}$ decreased as Λ increased. $[\Lambda_{450}]$ induced approximately 3x faster spectroscopic response than that induced by $[\Lambda_{525}]$ and more than 9x faster response than that induced by $[\Lambda_{625}]$. The proportionality may be explained by the higher photon energy at 450 nm and the different quantum efficiency in absorption at different λ. In addition to Λ, RH was also found to have significant effect on $k_{\Delta RN}$. ANOVA confirmed these observations and additionally suggested that the interaction between RH and Λ and the interaction between RH and $[O_2]$ were likely to be significant. For a clear-cut picture of the effects of these interactions, it would be desirable to carry out replication of the experimental runs for improved precision of the estimations of the effects and the errors. In most cases, consistent results were obtained for tristimulus analyses. However, the tristimulus transformation was found to have introduced biases to the quantitative assessment of the relative strength of different radiation and needs further investigation.

Declarations

Availability of data and materials: The datasets used and/or analysed during the current study are available included in the Supplementary Materials or from the corresponding author on reasonable request. **Funding:** This research was generously supported by the Engineering and Physical Sciences Research Council (EPSRC) Centre for Doctoral Training in Science and Engineering in Arts, Heritage and Archaeology (SEAHA), UK and the Smithsonian's Museum Conservation Institute Trust Funds, USA. **Acknowledgements**: The authors would like to acknowledge the support by UCL Institute for Sustainable Heritage (UK), the Smithsonian's Museum Conservation Institute (USA), The National Archives (UK) and Lichtblau e.K. (Germany). **Author contributions:** Y. L.: conceptualisation, formal analysis, investigation, methodology, software, validation, writing – original draft preparation. T. F.: conceptualisation,

methodology, supervision, writing – review & editing. M.S.: conceptualisation, methodology, resources, supervision, writing – review & editing. **Competing interests:** The authors declare that they have no competing interests.

References

Beneto, A. J. and Siva, A. (2017) 'Highly selective colorimetric detection of cyanide anions in aqueous media by triphenylamine and phenanthro(9,10-d)imidazole based probes', *Photochemical and Photobiological Sciences*. Royal Society of Chemistry, 16(2), pp. 255–261. doi: 10.1039/c6pp00345a.

Blades, N. *et al.* (2017) 'New tools for managing daylight exposure of works of art: case study of Hambletonian, Mount Stewart, Northern Ireland', *Journal of the Institute of Conservation*. Taylor & Francis, 40(1), pp. 15–33. doi: 10.1080/19455224.2016.1214610.

Brigham, R. *et al.* (2018) 'Colour Analysis Crowdsourcing as an Analytical Method : Metrology of Smartphone Measurements in Heritage Science', *Angewandte Chemie International Edition*, 57, pp. 7423–7427. doi: 10.1002/anie.201801743.

BSI (2012) *Specification for managing environmental conditions for cultural collections PAS 198:2012*. BSI Standards Limited 2012.

BSI (2014) *BSI Standards Publication Textiles — Tests for colour fastness Part B01 : Colour fastness to light : Daylight*.

Cave, G. C. B. and Hume, D. N. (1952) 'Colorimetric Determination of Silver with p-Dimethylaminobenzalrhodanine', *Analytical Chemistry*, 24(9), pp. 1503–1505. doi: 10.1021/ac60069a041.

CIE (2001) *Improvement To Industrial Colour- Difference Evaluation*. Vinenna.

Daniel, C. (1959) 'Use of Half-Normal Plots in Interpreting Factorial Two-Level Experiments', *Technometrics*, 1(4), pp. 311–341.

Díaz Hidalgo, R. J. *et al.* (2018) 'New insights into iron-gall inks through the use of historically accurate reconstructions', *Heritage Science*. Springer International Publishing, 6(1), pp. 1–15. doi: 10.1186/s40494-018-0228-8.

Dische, Z. (1953) 'Qualitative and quantitative colorimetric determination of heptoses', *Journal of Biological Chemistry*, 204, pp. 983–998.

Ford, B. (2014) 'The accelerated light fading of iron gall inks in air, hypoxia and near-anoxia', *ICOM-CC 17th Triennial Conference Preprints*, (Iii), p. art. 0604.

Gervais, C. *et al.* (2013) 'Why does Prussian blue fade? Understanding the role(s) of the substrate', *Journal of Analytical Atomic Spectrometry*, 28(10), pp. 1600–1609. doi: 10.1039/c3ja50025j.

Gervais, C. *et al.* (2014) 'Light and anoxia fading of Prussian blue dyed textiles', *Heritage Science*, 2(1), pp. 2–9. doi: 10.1186/s40494-014-0026-x.

Gervais, C. *et al.* (2015) 'X-ray Photochemistry of Prussian Blue Cellulosic Materials: Evidence for a

Substrate-Mediated Redox Process', *Langmuir*, 31(29), pp. 8168–8175. doi: 10.1021/acs.langmuir.5b00770.

Gervais, C. *et al.* (2016) 'Time resolved XANES illustrates a substrate-mediated redox process in Prussian blue cultural heritage materials', *Journal of Physics: Conference Series*, 712(1), pp. 4–8. doi: 10.1088/1742-6596/712/1/012139.

Gray, V. E. and Wright, J. R. (1964) 'Measurement of Photochemical Degradation in Certain Plastics by Color Reactions with Phenylenediamines', *Journal of Applied Polymer Science*, 8, pp. 1505–1519.

Grove, D. M. and Davis, T. P. (1992) *Engineering, Quality and Experimental Design*. New York: John Wiley & Sons, Inc.

Hofenk de Graaff, J. H., Roelofs, W. G. and van Bommel, M. (2004) 'Gallotannin dyestuffs', in Hofenk de Graaff, J. H. and Roelofs, W. G. (eds) *The Colourful Past: The Origins, Chemistry and Identification of Natural Dyestuffs*. Archetype Publications Ltd, pp. 286–294.

Hone, D. C., Haines, A. H. and Russell, D. A. (2003) 'Rapid, quantitative colorimetric detection of a lectin using mannose-stabilized gold nanoparticles', *Langmuir*, 19(17), pp. 7141–7144. doi: 10.1021/la034358v.

Del Hoyo-Meléndez, J. M. and Mecklenburg, M. F. (2011) 'The use of micro-fading spectrometry to evaluate the light fastness of materials in oxygen-free environments', *Spectroscopy Letters*, 44(2), pp. 113–121. doi: 10.1080/00387011003786050.

ICOM-CC and IIC (2014) *Environmental Guidelines ICOM-CC and IIC Declaration*. Available at: http://www.icom-cc.org/332/-icom-cc-documents/declaration-on-environmental-guidelines/#.YTkEINNKibs (Accessed: 8 September 2021).

Johnston-Feller, R. (2001) *Color Science in the Examination of Museum Objects: Nondestructive Procedures*. Los Angeles: The Getty Conservation Institute. doi: http://dx.doi.org/10.1016/j.iccn.2008.05.004.

Kirby, J. and Saunders, D. (2004) 'Fading and colour change of Prussian blue: Methods of manufacture and the influence of extenders', *National Gallery technical bulletin*, 25, pp. 73–99.

Koestler, D. *et al.* (2018) 'Does argon anoxia cause a color change in Prussian blue pigment?', *Journal of the American Institute for Conservation*. Taylor & Francis, 57(1–2), pp. 47–61. doi: 10.1080/01971360.2018.1478534.

Kolar, J. *et al.* (2006) 'Historical iron gall ink containing documents - Properties affecting their condition', *Analytica Chimica Acta*, 555(1), pp. 167–174. doi: 10.1016/j.aca.2005.08.073.

Korifi, R. *et al.* (2013) 'CIEL*a*b* color space predictive models for colorimetry devices – Analysis of perfume quality', *Talanta*, 104, pp. 58–66. doi: 10.1016/j.talanta.2012.11.026.

Lerwill, A. *et al.* (2015) 'Photochemical colour change for traditional watercolour pigments in low oxygen levels', *Studies in Conservation*, 60(1), pp. 15–32. doi: 10.1179/2047058413Y.0000000108.

Liu, Y., Fearn, T. and Strlič, M. (2021a) 'Dose-response Modelling for the Discolouration of Iron Gall Ink on

Paper', in Bridgland, J. (ed.) *Transcending Boundaries: Integrated Approaches to Conservation. ICOM-CC 19th Triennial Conference Preprints, Beijing, 17–21 May 2021*. Paris: International Council of Museums.

Liu, Y., Fearn, T. and Strlič, M. (2021b) 'Factorial Experimentation on Photodegradation of Historical Paper by Polychromatic Visible Radiation', *Heritage Science*, In press.

Liu, Y., Fearn, T. and Strlič, M. (2021c) 'Spectral sensitivity of the discoloration of Historical rag paper', *Talanta Open*, 4(100058). doi: 10.1016/j.talo.2021.100058.

Mahy, M., Van Eycken, L. and Oosterlinck, A. (1994) 'Evaluation of Uniform Color Spaces Developed after the Adoption of CIELAB and CIELUV', *Color Research & Application*, 19(2), pp. 105–121. doi: 10.1111/j.1520-6378.1994.tb00070.x.

Perron, N. R. and Brumaghim, J. L. (2009) 'A review of the antioxidant mechanisms of polyphenol compounds related to iron binding', *Cell Biochemistry and Biophysics*, 53(2), pp. 75–100. doi: 10.1007/s12013-009-9043-x.

Reißland, B. and Cowan, M. W. (2002) 'The light sensitivity of iron gall inks', *Works of art on paper: books, documents and photographs: techniques and conservation: contributions to the Baltimore Congress, 2-6 September 2002*, (Iii), pp. 180–184.

Reißland, B. and Groot, S. De (1999) 'Ink corrosion comparison of currently used aqueous treatments for paper objects.pdf', in *Preprint from the 9th International Congress of IADA, Copenhagen, August 15-21*, pp. 121–130.

Rosu, D., Rosu, L. and Cascaval, C. N. (2009) 'IR-change and yellowing of polyurethane as a result of UV irradiation', *Polymer Degradation and Stability*. Elsevier Ltd, 94(4), pp. 591–596. doi: 10.1016/j.polymdegradstab.2009.01.013.

Rouchon, V. *et al.* (2011) 'Room-Temperature Study of Iron Gall Ink Impregnated Paper', *Analytical Chemistry*, 83(7), pp. 2589–2597.

Saunders, D. and Kirby, J. (1994) 'Studies in Conservation Wavelength-dependent fading of artists ' pigments WAVELENGTH-DEPENDENT FADING OF ARTISTS ' PIGMENTS', *Studies in Conservation*, 39, pp. 190–194. doi: 10.1179/sic.1994.39.Supplement-2.190.

Savitzky, A. and Golay, M. J. E. (1964) 'Smoothing and Differentiation of Data by Simplified Least Squares Procedures', *Analytical Chemistry*, 36(8), pp. 1627–1639. doi: 10.1021/ac60214a047.

Sharma, G., Wu, W. and Dalal, E. N. (2005) 'The CIEDE2000 Color-Difference Formula: Implementation Notes, Supplementary Test Data, and Mathematical Observations', *Color Research and Application*, 30(1), pp. 21–30. doi: 10.1002/col.20070.

Skoog, D. A. *et al.* (2012) *Fundamentals of Analytical Chemistry*. 9th edn. CA: Cengage Learning.

Smithsonian Institution Archives (no date) *Temperature and Humidity*. Available at: https://siarchives.si.edu/what-we-do/preservation/environment (Accessed: 8 September 2021).

Thomas, J. *et al.* (2010) 'A chemiluminescence study of madder lakes on paper', *Polymer Degradation and*

Stability, 95(12), pp. 2343–2349. doi: 10.1016/j.polymdegradstab.2010.08.024.

Tse, S. *et al.* (2010) 'Microfade Testing of 18th Century Iron Gall Inks', in Thompson, J. et al. (eds) *38th Annual Meeting of the American institute for Conservation of Historic and Artistic Works*, pp. 56–73.

Villmann, B. and Weickhardt, C. (2021) 'The Influence of Atmospheric Oxygen on the Color Change of Selected Historic Pigments and Dyes Caused by Narrow Band Optical Radiation', *Studies in Conservation*, 66(3), pp. 167–173.

Highlights

Iron gall ink mainly discolours at wavelength beyond 600 nm.

The discolouration is mainly affected by oxygen, relative humidity and their interaction.

Visible radiation in the blue region induces the fastest discolouration.

Declaration of interests

☒ The authors declare that they have no known competing financial interests or personal relationships that could have appeared to influence the work reported in this paper.

☐The authors declare the following financial interests/personal relationships which may be considered as potential competing interests: